Available online at www.sciencedirect.com
ScienceDirect
Journal of Photochemistry and Photobiology A: Chemistry 194 (2008) 1–10
Journal of Photochemistry and Photobiology A:Chemistry
www.elsevier.com/locate/jphotochem

Treatment of paper pulp and paper mill wastewater by coagulation–flocculation followed by heterogeneous photocatalysis

Angela Claudia Rodrigues, Marcela Boroski, Natalia Sueme Shimada, Juliana Carla Garcia, Jorge Nozaki ✠, Noboru Hioka *

Departamento de Química, Universidade Estadual de Maringá, Av. Colombo, 5790, CEP 87020-900 Maringá, PR, Brazil

Received 12 March 2007; received in revised form 26 June 2007; accepted 7 July 2007
Available online 12 July 2007

Abstract

In this work is investigated the combined treatment of post-bleaching effluent from a cellulose and paper industry. The biodegradability index determined by the biochemical oxygen demand (BOD)/chemical oxygen demand (COD) ratio of in natura sample was 0.11, which implies little biodegradability and that it may not be discharged to the environment without previous treatment. First, the effluent was submitted to the coagulation–flocculation treatment applying $FeCl_3$ as the coagulating agent and chitosan as an auxiliary. In sequence, the aqueous soluble phase obtained from the first treatment was submitted to a $UV/TiO_2/H_2O_2$ system using mercury lamps. The optimized coagulation experimental conditions were chosen: pH 6.0, 80 mg L^{-1} of $FeCl_3{\cdot}6H_2O$, and 50 mg L^{-1} of chitosan. The optimized photocatalysis conditions were: pH 3.0 in 0.50 g L^{-1} of TiO_2 and 10 mmol L^{-1} of H_2O_2. COD values for the in natura sample was 1303 mg L^{-1} and after the optimized conditions of coagulation without chitosan and in chitosan presence were 545 and 516 mg L^{-1}, respectively. Effluent turbidity decreased sharply after coagulations (from 10 FTU of in natura samples to 2.5 FTU without chitosan and 1.1 FTU with chitosan). Similarly, a decrease was observed for concentrations of N-ammoniac, N-organic, nitrate, nitrite, phosphate, and sulfate ions after coagulation. Additionally, it was observed an absorbance reduction of 90% at the wavelength of 500 nm and of 70–80% in regions corresponding to aliphatic and aromatic groups (254, 280, and 310 nm). The use of chitosan for quantitative purposes was not so efficient; however, it improves sedimentation and compaction. COD results of photolyzed samples by UV/H_2O_2 were 344 mg L^{-1}, UV/TiO_2 326 mg L^{-1}, and $UV/TiO_2/H_2O_2$ 246 mg L^{-1}. The reduction in absorbance intensity was approximately 98% for aliphatic and aromatic chromophores, and 100% for chromophores absorbing at 500 nm with color disappearance. During photodegradation, SO_4^{2-} was formed (~340 mg L^{-1} for the coagulated sample to ~525 mg L^{-1}) suggesting again the mineralization of the pollutant. The combined method (coagulation followed by photocatalysis) resulted in a biodegradability index of 0.71, transparency, and absence of color and odor in the treated water, suggesting again good water quality. This result is reinforced by the toxicity studies employing *Artemia salina* bioassay, which showed that an expressive decrease in toxic pollutants in effluents after treatment, mainly by combined processes. The wastewater treatment carried out in association at optimized experimental conditions provided good results.

Keywords: Wastewater; Coagulation; $FeCl_3$; Photocatalysis; TiO_2

1. Introduction

The cellulose and paper industry employs large amounts of water [1–3], and produce equally large amounts of wastewater, which constitutes one of the major sources of aquatic pollution. The lignin and its derivatives contained in this residue may produce highly toxic and refractory compounds, some potentially mutagenic [4]. The largest volume of pollutants are produced in the cellulose pulp bleaching step, which generates several chlorinated compounds via chlorination, and others toxic organic compounds, including lignin-derived refractory ones. This pulp and paper mill wastewater is little biodegradable, with BOD/COD ratio (biochemical oxygen demand divided by chemical oxygen demand) values usually around 0.02–0.07 [5]. Research [6] reports that samples with biodegradability index smaller than 0.3 are not appropriate for biological degradation. According to Chamarro et al. [7], for complete biodegradation, the effluent must present a biodegradability index of at least 0.40.

* Corresponding author. Tel.: +55 44 3261 3656.
E-mail address: nhioka@uem.br (N. Hioka).
✠ In memoriam.

1010-6030/$ – see front matter © 2007 Elsevier B.V. All rights reserved.
doi:10.1016/j.jphotochem.2007.07.007

Coagulation–flocculation is one of the most used water effluent treatments. It employees a cationic metal as a coagulant agent that usually promotes water hydrolysis and the formation of hydrophobic hydroxide compounds with different charges, depending on the solution pH. It may also lead to the formation of polymeric compounds. The coagulant agents interact with colloidal materials by either charge neutralization or adsorption, leading to coagulation–flocculation usually followed by sedimentation [8]. Coagulation effectiveness and cost depend on coagulant type and concentration, solution pH, ionic strength, as well as both concentration and nature of the organic residues in effluent [9,10]. Additionally, natural and artificial polyelectrolytes can be employed as flocculation auxiliaries, thus enhancing the processes due to their ability to generate robust and dense flocks, which in turn may easily form stable and compact sediments [4]. Chitosan, a natural [11,12] non-toxic biodegradable polyelectrolyte [13–15], presents positive charges in acid medium due to its glucosamin units that interact and neutralize negatively charged surface particles, thus allowing their removal [16]. Several researchers have applied chitosan as a coagulant alone or associated with iron and aluminum salts [11,13,17–19].

A more complex effluent treatment is the advanced oxidation process (AOP) involving the conversion of organic pollutants to short species and even to their complete mineralization [20] through the generation of highly reactive free radical oxidants [21]. Some AOP techniques [22] are: H_2O_2, O_3 (ozonation), Fe(II)/Fe(III) with H_2O_2 (Fenton reaction), UV irradiation (direct photolysis), UV/H_2O_2, UV/catalyst/H_2O_2, UV/$\{$Fe(II)/Fe(III) + $H_2O_2\}$ (Photo-Fenton), UV/O_3 (photo-ozonation), and others. Photocatalysis is an important alternative because it can eliminate refractory residues (also known as photodegradation and photo-oxidation methods). However, according to Gogate and Pandit [23], for successful photocatalysis, COD values must be lower than 800 mg L^{-1} as high suspended material content leads to light scattering effects. At the same time, organic matter tends to recover the catalyst surface (adsorption), which could diminish the amount of photons that reaches photo-reactive sites on TiO_2 [24,25]. One alternative for wastewater treatment is to apply a physical–chemical procedure such as coagulation to eliminate most of the organic materials first, followed by photocatalysis as the second treatment.

UV/heterogeneous treatment using metal oxide semiconductors like TiO_2, ZnO, CeO_2, CdS, ZnS, and others [23] as a catalyst may generates large amounts of free radicals on the catalyst surface leading to the fast degradation of many refractory species, usually in larger amounts than by homogeneous photocatalysis. In addition, the heterogeneous system is a low cost technique [23,26]. Titanium dioxide is a catalyst widely employed in photocatalysis either in suspension [27] or immobilized [28]. It has low cost, is non-toxic, photo stable in a wide range of pH [29], recoverable after wastewater treatment, and adequate for industrial scale [23]. The solution/effluent pH is an important parameter in heterogeneous photocatalysis. It modulates the catalyst charge and consequently affects both pollutant adsorption and particle aggregation [30].

The photocatalytic reaction occurs when the semiconductor is activated by light. The light radiation energy should be equal or higher than those necessary to generate the band gap. For TiO_2, the band gap energy is 3.2 eV, which corresponds to absorption at wavelengths shorter than ca. 390 nm [29]. One electron is promoted from valence band (producing positive holes, h_{VB}^+) to conduction band (e_{CB}^-), as describes Eq. (1) [22]:

$$TiO_2 + h\nu \rightarrow TiO_2(e_{CB}^-) + TiO_2(h_{VB}^+) \quad (1)$$

In sequence there are some possibilities evolving adsorbed compounds at the catalyst surface by reaction with the roles h_{VB}^+ where they are oxidized. The h_{VB}^+ can oxidize adsorbed organic compounds directly leading them to degradation (Eq. (2)); the h_{VB}^+ can reacts with adsorbed water (Eq. (3)) and hydroxide ions (Eq. (4)) at the surface producing hydroxyl radicals ($HO^\bullet$). This radical is considered the main oxidant specie formed in the system. For the other hand, simultaneously the electron (e_{CB}^-) can reduce the adsorbed oxygen (Eq. (5)) producing hydroperoxyl radicals (Eq. (6)), hydrogen peroxide (Eq. (7)), more hydroxyl radicals (Eqs. (8) and (9)), and others [22,31]:

$$\text{Pollutants} + h_{VB}^+ \rightarrow \text{oxidized products} \quad (2)$$

$$h_{VB}^+ + H_2O \rightarrow HO^\bullet + H^+ \quad (3)$$

$$h_{VB}^+ + HO^- \rightarrow HO^\bullet \quad (4)$$

$$e_{CB}^- + O_2 \rightarrow O_2^{\bullet -} \quad (5)$$

$$O_2^{\bullet -} + H^+ \rightarrow HO_2^\bullet \quad (6)$$

$$2HO_2^\bullet \rightarrow H_2O_2 + O_2 \quad (7)$$

$$H_2O_2 + e_{CB}^- \rightarrow HO^\bullet + HO^- \quad (8)$$

$$H_2O_2 + O_2^{\bullet -} \rightarrow HO^\bullet + HO^- + O_2 \quad (9)$$

Additionally, hydrogen peroxide can absorb light and directly form hydroxyl radicals even in the absence of semiconductor. The organic compounds (pollutants) present in the medium react mainly with both hydroxyl and hydroperoxyl radicals; however, the degradation by hydroxyl radical is cited as the most effective in these systems. As hydrogen peroxide is an adequate source of hydroxyl radicals, the addition of this reagent to the system enhances the efficacy of the photocatalysis process [27,29,32,33].

In the present work, a combined treatment of coagulation–flocculation followed by heterogeneous photocatalysis is applied to cellulose and paper industry effluents. All samples were analyzed before and after each step. Optimal chemical compositions and experimental conditions were investigated for both processes. A bioassay using micro-crustacean *Artemia salina* was performed to certify water purity.

2. Experimental procedures

2.1. Materials

Titanium dioxide (TiO_2 P25, ca. 80% anatase, 20% rutile; BET area, ca. 50 $m^2\ g^{-1}$) was kindly supplied by Degussa Co.

(Brazil). The catalyst was used as received. All of the reagents used in this work were analytical grade and were used without any further purification.

Effluent samples were collected after cellulose pulp bleaching. Analytical determinations were carried out with in natura effluent and treated samples according to Standard Methods of Examination of Water and Wastewater [34]. BOD was determined by oxygen dosage measured initially and after incubation at 20 °C for 5 days, following the methodology described [34,35]. Values of COD were obtained by colorimetry after digestion by dichromate ion (known excess) in strong acid media [34]; both analysis were performed in triplicate. It was also obtained UV–vis molecular absorption spectra in a Varian-Cary 50 UV–vis spectrophotometer to monitor the reduction of absorbance at 254, 280, 310, and 500 nm, using 4 mL quartz cuvettes with 10 mm of optical path. The chosen wavelengths represent the chromophore groups of molecules: 254 nm corresponds to the aliphatic region; 280 nm is related to aromatic groups like phenols, which are usually present in this kind of effluent; 310 nm corresponds to conjugated aromatic rings; 500 nm represents visible light-absorbing molecules. pH (Tecnal-3MP) and turbidity (Micronal-B250) measurements were also performed. Coagulation–flocculation treatment was studied in jar test equipment (Milam, rpm, JT1010).

2.2. Coagulation–flocculation process

Coagulation–flocculation was conducted with $FeCl_3$ as a coagulant and chitosan as an auxiliary coagulant with stock solutions of 0.37 mol L^{-1} of $FeCl_3{\cdot}6H_2O$ and 1% (w/v) chitosan dissolved in 0.1 mol L^{-1} HCl. The experiments were performed in jar test using a sample volume of 1000 mL stirred (120 rpm) for 30 s followed by 15 min of slow agitation (20 rpm). After 30 min, flocks settled down at the bottom of the vessel and the aqueous phase was collected. Tests performed at various pH and $FeCl_3$ and chitosan concentrations allowed to optimize the process. In some cases, coagulation treatments were made with $FeCl_3$ alone (without chitosan).

2.3. Photo-oxidation process

The photocatalysis process was conducted with UV/TiO_2, UV/H_2O_2, and UV/TiO_2/H_2O_2 systems. The aqueous phase samples from the coagulation–flocculation treatment performed in optimized conditions in absence of chitosan were kept in a fridge. These samples were submitted to complementary photocatalysis treatment with artificial UV light irradiation provided by a 250 W low pressure mercury lamp without the glass bulb (Empalux) in the photo-reactor system described: 300 mL of effluent was placed in 600 mL borosilicate glass Erlenmeyers (3×) used as reaction vessels. The Erlenmeyers were placed in a wooden made box (80 cm × 50 cm) fit with three lamps on the top side 15 cm away from the samples. The light power was measured by a light meter apparatus (Newport Optical Power Meter Model 1830-C), with the wavelength set at 400 nm. Appropriate amounts of TiO_2 and H_2O_2 were added to the flask to achieve the concentrations wanted. The resulting TiO_2 suspension was stirred during irradiation (magnetic stirrer). Four fans fit on the box side walls were used to reduce the heat caused by the lamps. Photocatalyzed samples were filtered with membranes (Millipore, either 0.22 or 0.45 μm pore diameter) to isolate the treated water from TiO_2 and kept under refrigeration until analysis. The electronic absorption spectra were obtained to determine the level of degradation of the effluent. The mineralization of these compounds was verified by physical and chemical analysis. The residual peroxide after the irradiation was analyzed according to Silva et al. [36].

The pH optimization was carried out by using 0.50 g L^{-1} of TiO_2 at pH 3.0, 5.0, 7.0 and 10.0 adjusted with 0.10 mol L^{-1} HCl and 0.10 mol L^{-1} NaOH. Concentrations of 0.25, 0.50 and 0.75 g L^{-1} TiO_2 were used in tests at pH 3.0. To determine the optimum H_2O_2 quantity, effluent with 0.50 g L^{-1} TiO_2 at pH 3.0 was irradiated using different H_2O_2 concentrations (10, 50, and 75 mmol L^{-1}). The influence of heating on effluent degradation was studied. The Erlenmeyers were wrapped with aluminum foil (samples in the dark) and placed in the photo-reactor (heating control). In addition, experiments were performed using UV radiation (absence of H_2O_2 and TiO_2), UV/H_2O_2, and UV/TiO_2 for comparisons with the UV/TiO_2/H_2O_2 system results.

2.4. Biotoxicity method

Biotoxicity assays [37–39] with *A. salina* were performed as described [40]. Eggs were hatched in water containing NaCl (3.8 g L^{-1}) under weak white light (6 W) at room temperature. After 48 h, 20 crustaceans were transferred to test tubes. Samples were prepared by adding 0.5, 1.0, 1.5, 2.0, and 2.5 mL of effluent to the test tubes, which were filled up to 3 mL with saline water to produce samples of 17, 33, 50, 67, and 83% (v/v) of effluents. After 24 h, the number of surviving organisms in each tube was counted. All assays were carried out in triplicate accompanied by control tests.

3. Results and discussion

3.1. Coagulation–flocculation studies

3.1.1. Optimization of pH

At first, pH optimum operating conditions for effluent coagulation with $FeCl_3$ was evaluated using jar tests. To determine the quality of the final water under treatment, parameters such as turbidity, COD concentration, and percent absorbance reduction for chromophore groups in the UV and visible regions were utilized. The results are shown in Fig. 1.

According to the data in Fig. 1(A), the lowest remaining turbidity and COD values were observed at $5.5 < pH < 6.5$, which was confirmed by Tukey test with $P < 0.05$. Likewise, the best percent absorbance reduction was at $5.5 < pH < 6.5$ for chromophores in the UV region (Fig. 1(B)). For colored compounds (500 nm), the largest decrease in intensity occurred at pH <6.5, showing an efficacy higher than the one observed for UV absorbents. Therefore, the best pH chosen is 6.0 in this experimental condition.

At pH 5.0, the main Fe^{n+} species present in solution is $Fe(OH)_2^+$, while at pH around 8.0, it is $Fe(OH)_3$ [10]. $Fe(OH)_2^+$

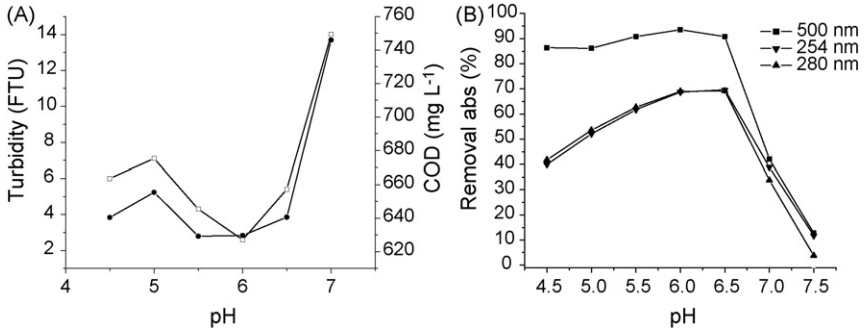

Fig. 1. pH influence on the coagulation of pulp and paper mill effluent: (A) turbidity values (□) and concentration (●) of COD. (B) Percent reduction of absorbance intensity at several wavelengths. Coagulation performed at 80.0 mg L^{-1} of $FeCl_3 \cdot 6H_2O$.

can neutralize negative charge density materials like organic substances and suspended particles [24]. On the other hand, $Fe(OH)_3$, a hydrophobic compound, can adsorb contaminants particles by surface interactions, which in some cases can lead to polymeric entities [41]. At the chosen pH 6.0, both compounds are present (mainly $Fe(OH)_2^+$), leading to pollutant aggregation and precipitation.

3.1.2. Optimization of $FeCl_3$ concentration

Chosen the adequate pH (pH 6.0), the best coagulant quantity was determined. Analytical data for the coagulated samples are presented in Fig. 2.

The data in Fig. 2(A) show that both the residual turbidity and COD values against coagulant concentration exhibit a very similar profile, similarly to that observed in Fig. 1(A) for both parameters. The profile for these two parameters, turbidity and COD values, shows a decrease as the coagulant concentration increases, exhibiting the highest effect for 80 mg L^{-1} of $FeCl_3 \cdot 6H_2O$ (Fig. 2(A)) as attested by Tukey test. For higher coagulant amounts, turbidity remained constant, meaning that an efficacy limit was reached; while for COD values, the performance decreases slightly. Similarly, the results in Fig. 2(B) show that the reduction of absorbents species at 254, 280, 310 (not shown) and 500 nm reached the highest removal at 80 mg L^{-1}, whose values became constant as the coagulant concentration was raised.

From these results it is clear that at pH 6.0, the assays with 80 mg L^{-1} of $FeCl_3 \cdot 6H_2O$ presented the best performance. Thus, this concentration was applied for the others experiments. Even though the use of high $FeCl_3$ quantities does not enhance process efficiency, therefore it allows coagulant saving.

3.1.3. Optimization of polyelectrolyte loading

Studies of chitosan as an auxiliary polyelectrolyte coagulant were conducted with 80.0 mg L^{-1} of $FeCl_3 \cdot 6H_2O$ and pH 6.0. The same analytical parameters previously used were employed to evaluate treated effluent (Fig. 3).

The results illustrated in Fig. 3(A) indicate that the largest decrease in turbidity occurred in experiments carried out with 25 and 50 mg L^{-1} of chitosan, while for COD reduction, it took 50 mg L^{-1} of chitosan. Absorbent reduction data showed that coagulant amounts of 50, 60, and 75 mg L^{-1} neared bleaching level for wavelengths corresponding to aliphatic and aromatic groups, while at 500 nm, coagulant amounts of 25 and 50 mg L^{-1} were the most efficient. Thus, 50 mg L^{-1} of polyelectrolyte was chosen as the optimized condition.

For comparison sake, the analytical results of samples in natura, after coagulation–flocculation treatments ($FeCl_3$ and pH 6.0) in the absence and in the presence of chitosan are presented in Table 1.

For convenience, in natura effluent data are also presented (Table 1). The calculated experimental biodegradability (ratio BOD/COD) is 0.11. For indexes below 0.3, it is known that the sample is not appropriate for biological degradation [6]. Moreover, for complete biodegradation, the effluent must present a biodegradability index of at least 0.40 [7]. At the same time, a COD concentration of 1303 mg L^{-1} indicates that the effluent is not suitable for photocatalysis treatment as the first method,

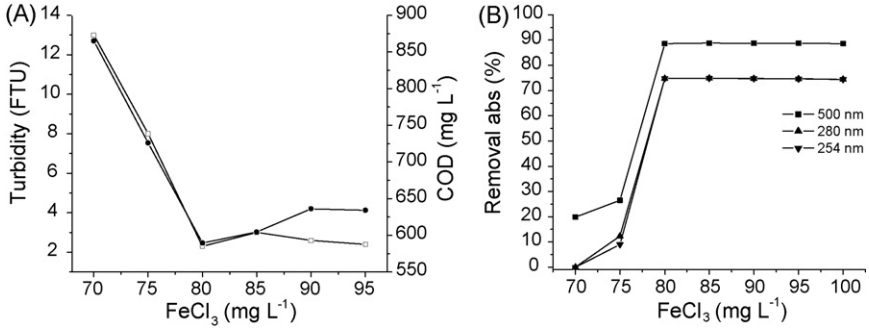

Fig. 2. Effects of $FeCl_3$ concentrations on final wastewater sample treated by coagulation at pH 6.0: (A) turbidity (□) and COD (●). (B) Percent reduction of absorbance intensity at several wavelengths.

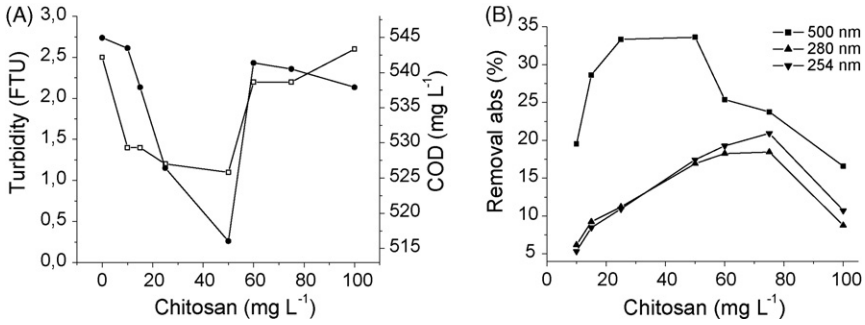

Fig. 3. Influence of chitosan concentration on coagulation: (A) turbidity (□) and COD (●) values. (B) Percent reduction of absorbance intensity at several wavelengths (calculated taking experimental value without chitosan as reference). All experiments were performed at 80.0 mg L^{-1} of $FeCl_3 \cdot 6H_2O$ and pH 6.0.

which requires a COD value lower than 800 mg L^{-1} for successful treatment [23]. As previously discussed, the turbidity and COD values decrease sharply after coagulation (Table 1). The same pattern is observed for all ions analyzed. The major anion in in natura wastewater is sulfate, resulting from Kraft technology. Its concentration fell by almost 50% after coagulation.

The statistical treatment on the data for the system with chitosan, Table 1, showed effluent purification improvement (values with different letters in the same line are different). Despite it, the chitosan performance is only moderate so that this auxiliary coagulant was not used in the next experiments. However in industrial scale applications, the use of polyelectrolytes may be interesting because they promote faster coagulation and better sedimentation, producing compact pollutant flocks.

The optimized coagulation–flocculation conditions are pH 6.0 and 80 mg L^{-1} of $FeCl_3 \cdot 6H_2O$. This process was used as the initial method to treat cellulose and paper industry wastewater. The aqueous phase obtained was submitted to a second step, the photocatalysis process.

3.2. Photocatalysis studies

The light source power inside the photo-reactor (3 × 250 W, mercury lamps) was measured with the light meter probe placed at the same position of the sample resulting in irradiance of approximately 8.9 mW cm^{-2}.

3.2.1. pH optimization

The effect of pH on photocatalysis efficiency was investigated employing TiO_2 in in natura effluent (diluted 1:1, v/v). The results are shown in Fig. 4.

The major percent reduction in absorbance and the lowest amount of remaining COD, parameters that indicate the highest efficiency, were obtained in the experiment photocatalyzed at pH 3.0. This result could be explained considering the zero charge point of the catalyst (pH_{pcz}), which occurs at pH 6.25 for TiO_2. As the surface is positively charged at pH values lower than 6.25 ($Ti–OH_2^+$), it allows the adsorption of water and hydroxide ions, generating hydroxyl radicals and other oxidizing species (Eqs. (3)–(9)). As the same time there are adsorption of organic substances and suspended materials on $Ti–OH_2^+$ surface by charge and surface intermolecular interactions. Pulp and paper mill effluent particles have negative charge density due to anionic suspended materials and the presence of oxygen, carboxyl, and other negative groups in organic molecules. Therefore, the pollutants react with radical species formed on the catalyst surface.

3.2.2. Optimization of TiO_2 concentration

The effluent coagulated in the first step was used in the photodegradation process at pH 3.0 in presence of different TiO_2 quantities (Fig. 5).

As shown in Fig. 5, TiO_2 increased the photo-reaction process efficiency, which can be noted by the increase in percent

Table 1
Analytical characteristics of effluents in natura, after coagulation (80.0 mg L^{-1} of $FeCl_3 \cdot 6H_2O$ and pH 6.0) and in the presence of chitosan (80.0 mg L^{-1} $FeCl_3 \cdot 6H_2O$, pH 6.0 and 50.0 mg L^{-1} chitosan)

Parameter	In natura	After coagulation	After coagulation chitosan
pH	9.8	4.3	4.2
Turbidity (F.T.U.)	10	2.5	1.1
COD[a] (mg L^{-1})	1303 ± 25a	545 ± 18b	516 ± 9c
BOD[a] (mg L^{-1})	148 ± 5	Not measured	Not measured
N-ammoniac[a] (mg L^{-1})	1.68 ± 0.00	ND	ND
N-organic[a] (mg L^{-1})	1.1	ND	ND
Nitrate[a] (μg L^{-1})	168.5 ± 13.5a	16.3 ± 0.4b	7.0 ± 0.5c
Nitrite[a] (μg L^{-1})	44.8 ± 0.3	ND	ND
Phosphate[a] (μg L^{-1})	871.6 ± 2.3a	14.4 ± 0.5b	10.4 ± 0.6c
Sulfate[a] (mg L^{-1})	677.6 ± 7.3a	341.1 ± 4.6b	271.0 ± 9.2c

Different letters in the same line imply values statistically different ($P < 0.05$ by Tukey test). ND, not detected—below detection limits.
[a] $n = 3$ samples analyzed.

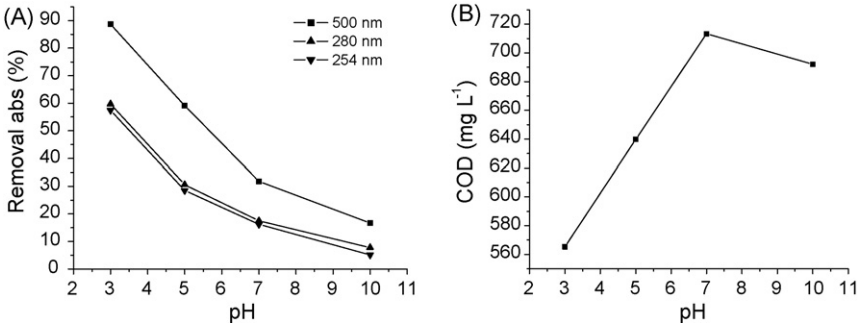

Fig. 4. Effect of pH on TiO_2 photocatalysis: (A) percent reduction of absorbance intensity at several wavelengths. (B) COD concentrations. Sample in natura diluted 1:1 (v/v), irradiated for 360 min in 0.50 g L^{-1} of TiO_2.

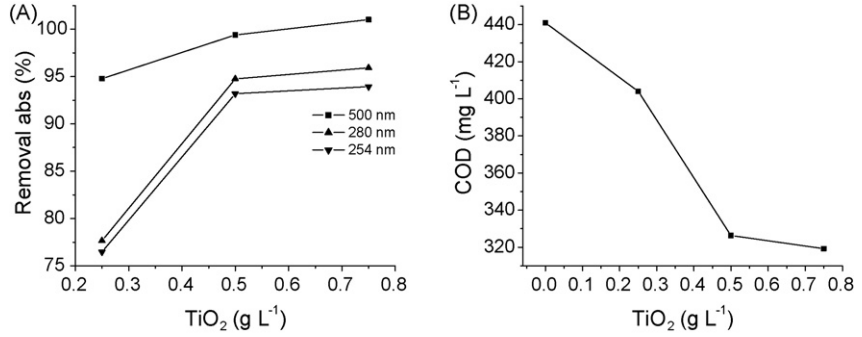

Fig. 5. Photocatalysis of coagulated samples: (A) percent reduction of absorbance intensity at several wavelengths. (B) COD concentrations. Effluent submitted to combined treatments. Step 1: 80 mg L^{-1} of $FeCl_3{\cdot}6H_2O$ and pH 6.0; step 2: irradiation for 360 min and pH 3.0.

absorbance removal and the decrease in COD values. For 0.50 g L^{-1} of catalyst, purification efficacy was slightly lower than that for 0.75 g L^{-1}; however, Tukey's test proved that the percent removal absorbance and COD values for these two TiO_2 concentrations are similar. Although the presence of the catalyst increases photo-oxidation yield, a high TiO_2 concentration does not necessarily imply a high reaction performance, at least in some regions with excess catalyst. The last experimental condition is not convenient for photodegradation because excess TiO_2 can cause strong turbidity effects, which make the passage of light throughout the heterogeneous solution difficult due to light scattering effects [22,23]. Therefore, TiO_2 concentration should be optimized for each effluent and system employed, because degradation efficiency depends on the nature and concentration of pollutants as well as on the level of free radicals generation, which is related to the photo-reactor operating conditions. In the present case, 0.50 g L^{-1} of TiO_2 and pH 3.0 were satisfactory.

3.2.3. *Optimization of H_2O_2 concentration*

The coagulated water sample was used to determine the optimum concentration of H_2O_2 to be employed in photocatalysis. The optimization studies were developed with 360 min of photodegradation time, 0.50 g L^{-1} of TiO_2, and pH 3.0. The results are illustrated in Fig. 6.

At the monitored wavelengths (except in visible region), the percent absorbance removal undergoes a small increase (from ~93 to ~99%) with the addition of 10 mmol L^{-1} of H_2O_2. However, this parameter remains constant for further increases to 50 and 75 mmol L^{-1} of H_2O_2 (Fig. 6(A)). The values of remaining

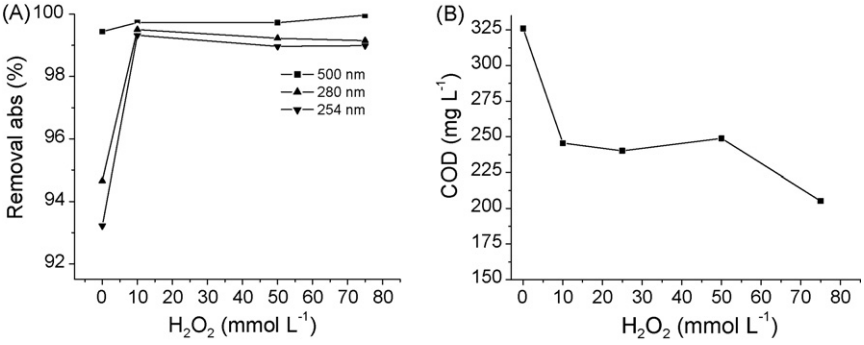

Fig. 6. Effect of H_2O_2 concentration on photodegradation efficiency: (A) percent reduction of absorbance intensity at several wavelengths. (B) COD concentration. Effluent submitted to combined treatments. Step 1: 80 mg L^{-1} of $FeCl_3{\cdot}6H_2O$ and pH 6.0; step 2: irradiation for 360 min, 0.50 g L^{-1} of TiO_2 and pH 3.0.

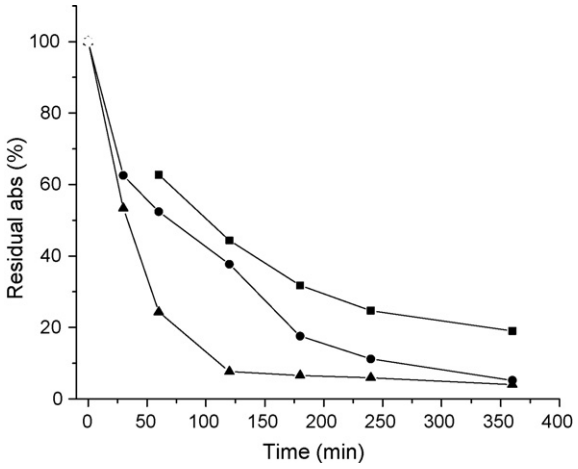

Fig. 7. Effects of TiO_2 and H_2O_2 on photo-reaction. Residual absorbance monitored at 280 nm as a function of irradiation time. Sample: effluent coagulated; photocatalysis at pH 3.0 with: (■) 10 mmol L^{-1} H_2O_2 (without TiO_2); (●) 0.50 g L^{-1} TiO_2 (without H_2O_2); (▲) 0.50 g L^{-1} TiO_2 and 10 mmol L^{-1} H_2O_2.

COD (Fig. 6(B)) decreased in the presence of H_2O_2 (higher efficacy); however, at 10, 25, and 50 mmol L^{-1} H_2O_2, the results were much similar (COD ~247 mg L^{-1}), with a change for 75 mmol L^{-1} H_2O_2, COD ~205 mg L^{-1}. However, these values are not proportional to the increase in H_2O_2 concentration (50–75 mmol L^{-1}, 50% increment). Some authors [33] state that in some circumstances hydrogen peroxide may prejudices heterogeneous photocatalysis by direct H_2O_2 absorption light, thus diminishing TiO_2 photo-excitation. Another possibility is that part of the hydroxyl radical is annihilated by excess H_2O_2, converting it to hydroperoxyl radical ($HO_2^{\bullet}$), which is suppressed by other hydroxyl radical producing $H_2O + O_2$. Therefore, the production of hydroxyl radical decreases as consequence of the high amount of H_2O_2 in solution.

The H_2O_2 concentration adopted in the next experiments was 10 mmol L^{-1} at 0.50 g L^{-1} of TiO_2 and pH 3.0. Analysis of the residual peroxide during the reaction indicated its clearance after 40 min of irradiation, which is very important, because peroxide residues in wastewater are hazardous to the environment.

3.2.4. Comparison of photo-reaction conditions

Fig. 7 shows the results for photocatalysis carried out with optimized quantities of TiO_2/H_2O_2, and pH, as well as the photocatalysis results obtained in the presence of the H_2O_2 and in the presence of TiO_2. Treatment efficiency was analyzed by absorbance in the 280 nm region, which is related to aliphatic and aromatic groups, including phenols.

As can be observed in Fig. 7, even the UV/H_2O_2 system promoted photodegradation, which occurred by direct H_2O_2 photo-excitation followed by oxidation. Direct H_2O_2 photo-reaction is limited by the need of light at 254 nm and the low absorption coefficient of H_2O_2 at this wavelength. Experiments carried out only with UV light showed that after 360 min of irradiation, the remaining absorbance at 280 nm was 32% (not shown), while for UV/H_2O_2, it was 20%, which implies that hydrogen peroxide improves the homogeneous photo-oxidation. However, the data (Fig. 7) show that while both UV/TiO_2/H_2O_2 and UV/TiO_2 systems lead to almost complete absorbance removal after 360 min irradiation (a 94% decrease when compared to coagulated effluent), the UV/H_2O_2 system is not so efficient. Although the UV/TiO_2 system shows similar absorbance removal values at 280 nm in presence and in the absence of H_2O_2, H_2O_2 clearly increases the absorbance removal velocity.

Table 2
UV-photolysis data of COD and percent COD removal calculated by comparison to coagulated and in natura samples

	COD[a] (mg L^{-1})	COD removal (calculated against coagulated) (%)	COD removal (calculated against in natura) (%)
UV	441a ± 14	19	66
UV + H_2O_2	344b ± 2	37	74
UV + TiO_2	326c ± 4	40	75
UV + H_2O_2 + TiO_2	246d ± 1	55	81

Irradiation at pH 3.0 and 0.50 g L^{-1} of TiO_2 and 10 mmol L^{-1} of H_2O_2. Different letters in the same column imply values statistically different ($P < 0.05$ by Tukey tests).

[a] $n = 3$ samples analyzed.

Table 2 contains COD determinations for experiments after photodegradation and percent COD reductions calculated by comparison to after-coagulation and in natura sample values, 545 and 1303 mg L^{-1}, respectively, for different photolysis systems. Irradiated samples were previously treated by coagulation).

The COD results in Table 2 show that all photosystems lead to pollutant degradation. The efficiency improvement follows the order: UV < UV/H_2O_2 < UV/TiO_2 < UV/TiO_2/H_2O_2, which agree with absorbance reduction results. However, the presence of H_2O_2 on TiO_2 improved degradation reasonably (from 40 to 55%), an effect not observed on the decrease in absorbance at 280 nm; part of the organic matter degradation, expressed by COD removal, may form products absorbing at this wavelength.

In respect to possible degradation reactions in samples submitted to high temperatures in the dark, it was observed that at 55 °C (the averaged temperature in the photo-reactor), the thermal reaction did not occur. This result is similar with the literature [23].

3.2.5. Kinetic studies of photodegradation

The absorption intensities during the irradiation of the UV/TiO_2 and UV/TiO_2/H_2O_2 systems monitored at several wavelengths, such as at 280 nm, Fig. 7, were submitted to kinetics mathematical treatment. Despite the low number of experimental points, the data reasonable obeyed the first-order kinetic law (Fig. 8) and showed no order changes for different experimental conditions, which agrees with the literature [32].

The observed first-order kinetic constants (k) and the half-life time ($t_{1/2}$) for both systems were exhibited in Table 3.

The k and $t_{1/2}$ values reinforced previous qualitative results, showing that hydrogen peroxide accelerates the photo-oxidation process over twofold. The photo-reaction of each system showed almost the same kinetic parameters at all wavelengths monitored in the UV region. However, for both photolysis systems, the data

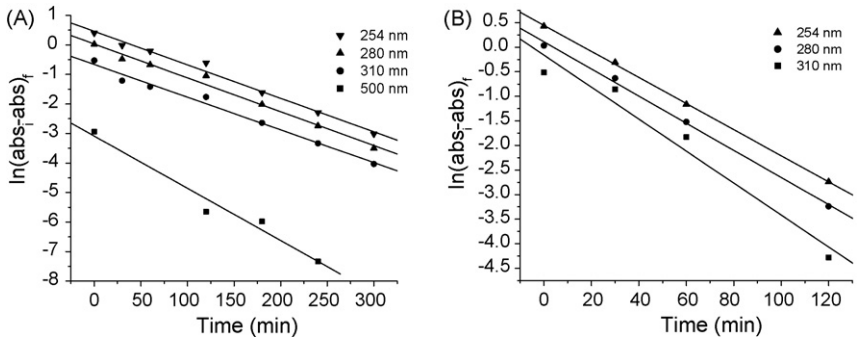

Fig. 8. Application of first-order kinetic law to photodegradation data at pH 3.0 in the presence of: (A) 0.50 g L^{-1} of TiO_2; (B) 0.50 g L^{-1} of TiO_2 and 10 mmol L^{-1} of H_2O_2.

Table 3
Correlation coefficients values (CC), k and $t_{1/2}$ for effluent irradiated at pH 3.0 in TiO_2 and TiO_2/H_2O_2 systems

	TiO_2 (0.50 g L^{-1})				TiO_2 (0.50 g L^{-1}) + H_2O_2 (10 mmol L^{-1})		
	254 nm	280 nm	310 nm	500 nm	254 nm	280 nm	310 nm
CC	0.994	0.994	0.993	0.985	0.999	0.999	0.981
k ($\times 10^{-2}$ min^{-1})	1.1	1.1	1.1	1.8	2.7	2.8	3.3
$t_{1/2}$ (min)	63	63	63	39	26	25	21

obtained at 500 nm show faster reaction than the ones monitored at UV region; for the UV/TiO_2/H_2O_2 system, the kinetics at 500 nm was too fast to be followed. Probably, the high electronic density of the chromophore unit (aromatic rings in high conjugation/resonance) that absorbs light in visible regions is more susceptible to fast attack by the photo-generated free radicals. The absorption at 254, 280 and 310 nm, wavelengths which is related to aliphatic region, aromatic ring (phenol groups) and restrict conjugated aromatic ring, respectively, correspond to groups which present lower electronic density, leading to photoreaction velocity slower than that one at 500 nm. However the kinetic studies performed by absorbance measurements can give information only for determined wavelengths that do not cover all the compounds present in the solution. Therefore it would be better to use TOC measurements that permit to obtain more complete information about complete organic mineralization for both, kinetic and photodegradation yielding (not performed experiments).

In Fig. 9 it is presented data on the sulfate ions formation and COD decay during irradiation. Sulfate ion appearance, at this step produced by organic matter decomposition, is very fast in the first 60 min. The COD variation profile was similar to that of absorbance decay.

3.3. Combined treatment (coagulation–flocculation and photocatalysis): effluent quality

A summary of the quality of in natura effluent sample, the coagulation–flocculation treated ($FeCl_3$) sample, and of the sample treated by combination coagulation followed by photo-oxidation (UV/TiO_2/H_2O_2) is analyzed as a function of absorbance intensity, and COD and ion concentrations. The experiments were conducted in optimized conditions (coagulation with 80 mg L^{-1} of $FeCl_3 \cdot 6H_2O$ at pH 6.0 and photocatalysis

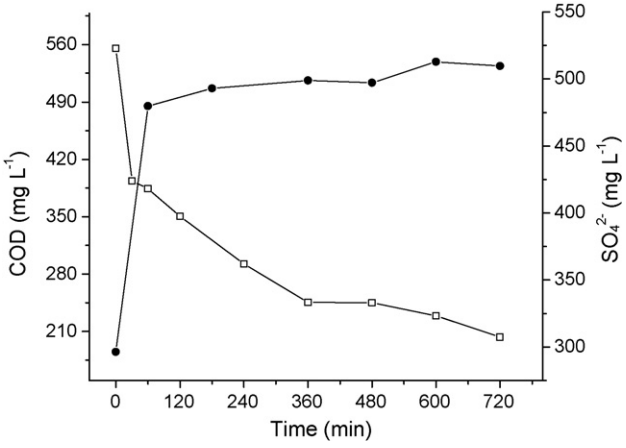

Fig. 9. Coagulated effluent submitted to irradiation in 0.50 g L^{-1} of TiO_2, 10 mmol L^{-1} of H_2O_2 and pH 3.0: (□) COD concentrations decrease; (●) appearance of SO_4^{2-}.

with 0.50 g L^{-1} of TiO_2, 10 mmol L^{-1} of H_2O_2, pH 3.0 at 360 min of irradiation). The photographs in Fig. 10 show the remaining samples color.

As can be seen, the brown color of the in natura effluent partially remained in the coagulated sample and was clarified in the final treated water. Coagulation reduced absorbance around 70–80% in wavelengths associated to aromatic and aliphatic groups (254, 280, and 310 nm), while in the combined treatment, removal was over 98% when compared to that of in natura effluent. The COD value of in natura effluent was 1303 mg L^{-1}; after coagulation, it decreased to 545 mg L^{-1} and after the combined treatment it fell to 246 mg L^{-1}. The concentrations of NO_3^- and PO_4^{3-} in effluent before and after photodegradation showed no significant changes (~16 and ~14 μg L^{-1}, respectively). As previously informed, NH_3 and NO_2^- were eliminated by the

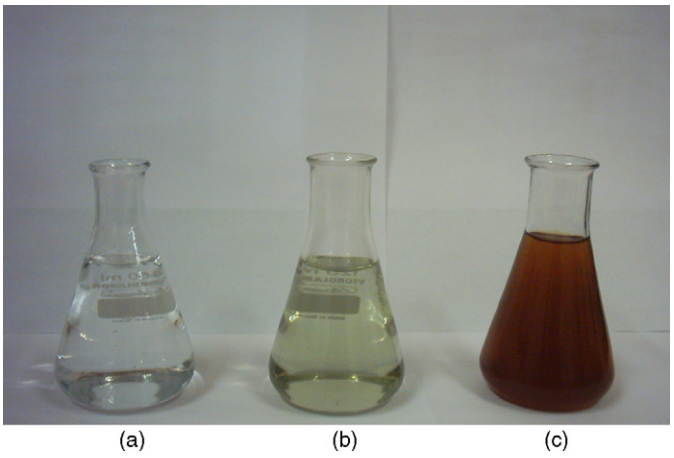

Fig. 10. Photograph of samples analyzed: (a) after combined treatment; (b) after coagulation; (c) in natura.

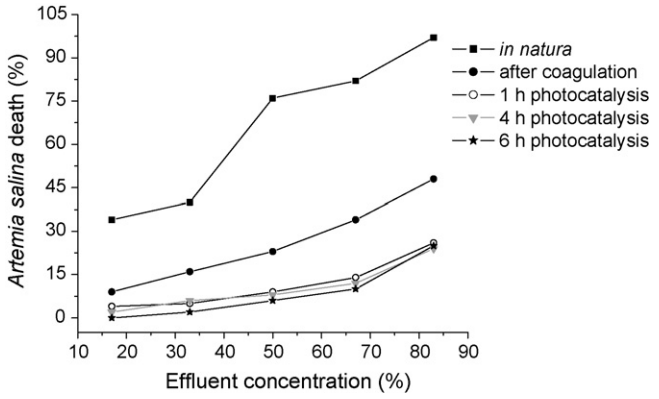

Fig. 11. Percent death of *Artemia salina* for samples: in natura, after coagulation, and combined coagulation-photodegradation for several irradiations time. All solutions were neutralized to pH ~7 before bioassay. The untreated effluent was diluted with aqueous NaCl, 3.8 g L^{-1} (v/v).

coagulation–flocculation process (step 1). These ions are not produced during photocatalysis. However, the quantity of sulfate ions changed from 678 mg L^{-1} (in natura) to 341 mg L^{-1} (coagulated sample) to 525 mg L^{-1} (after photocatalysis). Part of the sulfate ions is removed by coagulation and the remaining sulfated organic molecules are degraded during irradiation, indicating the mineralization process. Similarly, the increase in ionic solution conductivity after photo-reaction reinforced the mineralization direction (data not shown). Although total mineralization did not take place, these data pointed out that the inorganic compounds and organic pollutants were removed and/or degraded to simpler compounds.

Additionally, another in natura effluent sample was treated by the coagulation followed by photocatalysis in optimized conditions. Values of COD, BOD and biodegradability results are shown in Table 4.

The sample treated by coagulation showed a strong decrease in COD (around 56%) and a biodegradability index equal 0.50 (higher than 0.40), which means that the effluent can undergo complete biodegradation [7]. The COD of the coagulated sample, 514 mg L^{-1}, is lower than 800 mg L^{-1}, which allowed to infer the success of the photocatalysis process. The association of coagulation with 2 and 4 h of photocatalysis lead to biodegradability index of 0.63 and 0.71, respectively. These results are very positive, confirming the high level of elimination of pollutants from wastewater and that biological treatment in the next step may result in complete organic mater degradation.

These results indicate that the water quality is improved removing materials by coagulation followed by the conversion of pollutants to simpler and biodegradable compounds applying photocatalysis. However, some of the residues formed may be hazardous to aquatic environment. Therefore, biotoxicity experiments were carried out.

Table 4
Chemical and biochemical oxygen demand values and biodegradability index

Sample	COD (mg L^{-1})[a]	BOD (mg L^{-1})[a]	BOD/COD
In natura	1162 ± 3	172 ± 1	0.14
After coagulation	514 ± 14	257 ± 3	0.50
After 2 h photocatalysis	204 ± 7	129 ± 2	0.63
After 4 h photocatalysis	205 ± 6	145 ± 2	0.71

[a] $n = 3$ samples analyzed.

Bioassay results of all effluents (in natura and treated in optimized conditions) using *A. salina* are illustrated in Fig. 11.

Independently of effluent concentration, the index of *A. salina* mortality decreased after effluent coagulation for all sample treatments and was improved by photocatalysis purification. Photodegradation efficacy showed to be almost the same, independently of irradiation time, being 1 h seemingly sufficient. As an example, at 83% effluent, the mortality index in in natura sample was 97%, while in coagulated effluent, it was 50% and in photocatalyzed water, it was around 25%, the highest survival index.

These results demonstrate that the combined coagulation/photodegradation method investigated to treat pulp and paper mill effluents may be used to reduce water toxicity by the removal and/or degradation of pollutants.

4. Conclusion

The best experimental conditions were obtained for both processes. The first treatment step, coagulation–flocculation using $FeCl_3$ as a coagulant agent, eliminated several impurities from water efficiently, allowing the replacement of aluminum salts, which may be hazardous health [8,17]). Although the reduction of turbidity in chitosan presence was observed, this auxiliary coagulant did not contribute significantly to decrease COD and absorbance. However chitosan improves sedimentation velocity and compaction.

The addition of hydrogen peroxide to the UV/TiO_2 system did not enhance degradation yields substantially; however it increased the photo-process velocity. UV/TiO_2/H_2O_2 was more efficient than UV/TiO_2, UV/H_2O_2 and UV were.

The combined method reduced the organic charge and the inorganic pollutant species in effluent with good results. The biodegradability index for effluent submitted to coagulation–flocculation followed by photocatalysis showed that the final sample is suitable for complete biological degrada-

tion. The experimental application of the combined treatments to cellulose and paper industry effluents exhibited promising large-scale perspectives.

Acknowledgements

The authors wish to thank Dr. Edivaldo Egea Garcia for helping in manuscript preparation. This work was sponsored by Brazilian agencies Fundação Araucária, CNPq, and CAPES.

References

[1] S. Lacorte, A. Latorre, D. Barceló, A. Rigol, A. Malmqvist, T. Welander, Trends Anal. Chem. 22 (10) (2003) 725–737.
[2] D. Pokhrel, T. Viraraghavan, Sci. Total Environ. 333 (2004) 37–58.
[3] C.V. Srivastava, I.D. Mall, I. Mishra, Coll. Surf. A 260 (2005) 17–28.
[4] S.S. Wong, T.T. Teng, A.L. Ahmad, A. Zuhairi, G. Najafpour, J. Hazard. Mater. B 135 (2006) 378–388.
[5] G. Thompson, J. Swain, M. Kay, C.F. Forster, Bioresour. Technol. 77 (2001) 275–286.
[6] J.L. Morais, C. Sirtori, P.G. Peralta-Zamora, Quím. Nova 29 (1) (2006) 20–23.
[7] E. Chamarro, A. Marco, S. Esplugas, Water Res. 35 (4) (2001) 1047–1051.
[8] R.J. Stephenson, S.J.B. Duff, Water Res. 30 (4) (1996) 781–792.
[9] S. Delgado, F. Diaz, D. Garcia, N. Otero, Filtr. Sep. Sep. (2003) 43–46.
[10] J. Duan, J. Gregory, Adv. Coll. Interf. 100 (102) (2003) 475–502.
[11] A. Pinotti, A. Bevilacqua, N. Zaritzky, J. Food Eng. 32 (1997) 69–81.
[12] R. Divakaran, V.N.S. Pillai, Water Res. 35 (16) (2001) 3904–3908.
[13] S. Bratskaya, S. Schwarz, D. Chervonetsky, Water Res. 38 (2004) 2955–2961.
[14] H. Li, Y. Du, Y. Xua, H. Zhanb, J.F. Kennedyc, Carbohydr. Polym. 58 (2004) 205–214.
[15] R. Divakaran, V.N.S. Pillai, Water Res. 38 (2004) 2135–2143.
[16] A. Pinotti, N. Zaritzky, Waste Manage. 21 (2001) 535–542.
[17] R. Divakaran, V.N.S. Pillai, Water Res. 36 (2002) 2414–2418.
[18] J. Roussy, M.V. Vooren, D.A. Brian, E. Guibal, Water Res. 39 (2005) 3247–3258.
[19] S.P. Strand, T. Nordengen, K. Østgaard, Water Res. 36 (2002) 4745–4752.
[20] R. Andreozzi, V. Caprio, A. Insola, R. Marotta, Catal. Today 53 (1999) 51–59.
[21] A. Cuzzola, M. Bernini, P. Salvadori, Appl. Catal. B: Environ. 36 (2002) 231–237.
[22] M. Pera-Titus, V. García-Molina, M.A. Baños, J. Giméneza, S. Esplugas, Appl. Catal. B: Environ. 47 (2004) 219–256.
[23] P.R. Gogate, A.B. Pandit, Adv. Environ. Res. 8 (2004) 501–551.
[24] N. Daneshvar, D. Salari, A.R. Khataee, J. Photochem. Photobiol. A: Chem. 157 (2003) 111–116.
[25] M. Faisal, A.M. Tariq, M. Muneer, Dyes Pigments 72 (2007) 233–239.
[26] C.C. Chen, J. Mol. Catal. A: Chem. 264 (2007) 82–92.
[27] Y. Wang, C. Hong, Water Res. 33 (9) (1999) 2031–2036.
[28] N.M. Mahmoodi, M. Arami, N.Y. Limaee, N.S. Tabrizi, J. Coll. Interf. Sci. 295 (2006) 159–164.
[29] A.E.H. Machado, J.A. Miranda, R.F. Freitas, E.T.F.M. Duarte, L.F. Ferreira, Y.D.T. Albuquerque, R. Ruggiero, C. Sattler, L. Oliveira, J. Photochem. Photobiol. A: Chem. 155 (2003) 231–241.
[30] Y. Wang, C.S. Hong, F. Fang, Environ. Eng. Sci. 16 (1999) 433–440.
[31] P.A. Pekakis, N.P. Xekoukoulotakis, D. Mantzavinos, Water Res. 40 (2006) 1276–1286.
[32] C. Hachem, F. Bocquillon, O. Zahraa, M. Bouchy, Dyes Pigments 49 (2001) 117–125.
[33] W. Chu, C.C. Wong, Water Res. 38 (2004) 1037–1043.
[34] L.S. Clesceri, A.E. Greenberg, A.D. Eaton, Standard Methods for the Examination of Water and Wastewater, 20th ed., American Public Health Association, Washington, DC, USA, 1998.
[35] M.O.S.A. Silva, Análises físico-químicas para controle de estações de tratamento de esgotos, Companhia de Saneamento Ambiental CETESB, São Paulo, Brazil, 1977.
[36] M.R.A. Silva, M.C. Oliveira, R.F.P. Nogueira, Eclética Quím. 29 (2004) 19–26.
[37] J. Lindsay, J.S. Metcalf, G.A. Codd, Toxicon 48 (2006) 995–1001.
[38] J. Castritsi-Catharios, N. Bourdaniotis, G. Persoone, Chemosphere 67 (2007) 1127–1132.
[39] M. Favilla, L. Macchia, A. Gallo, C. Altomare, Food Chem. Toxicol. 44 (2006) 1922–1931.
[40] B.N. Meyer, N.R. Ferrigini, J.E. Putnan, L.B. Jacobsen, D.E. Nichols, J.L. McLaughlin, Planta Medica 45 (1982) 31.
[41] M.Y.A. Mollah, P. Morkovsky, J.A.G. Gomes, M. Kesmez, J. Parga, D.L. Cocke, J. Hazard. Mater. B 114 (2004) 199–210.